Lignin-based Film with Tunable Mechanical Properties Enabled by Polyether Amine Incorporation

Ruige Qi, Fei Song, Lihong Hu,* and Meng Zhang *

**Corresponding authors: zhangmeng@icifp.cn; hlh@icifp.cn*

DOI: 10.15376/biores.21.3.8528-8539

GRAPHICAL ABSTRACT

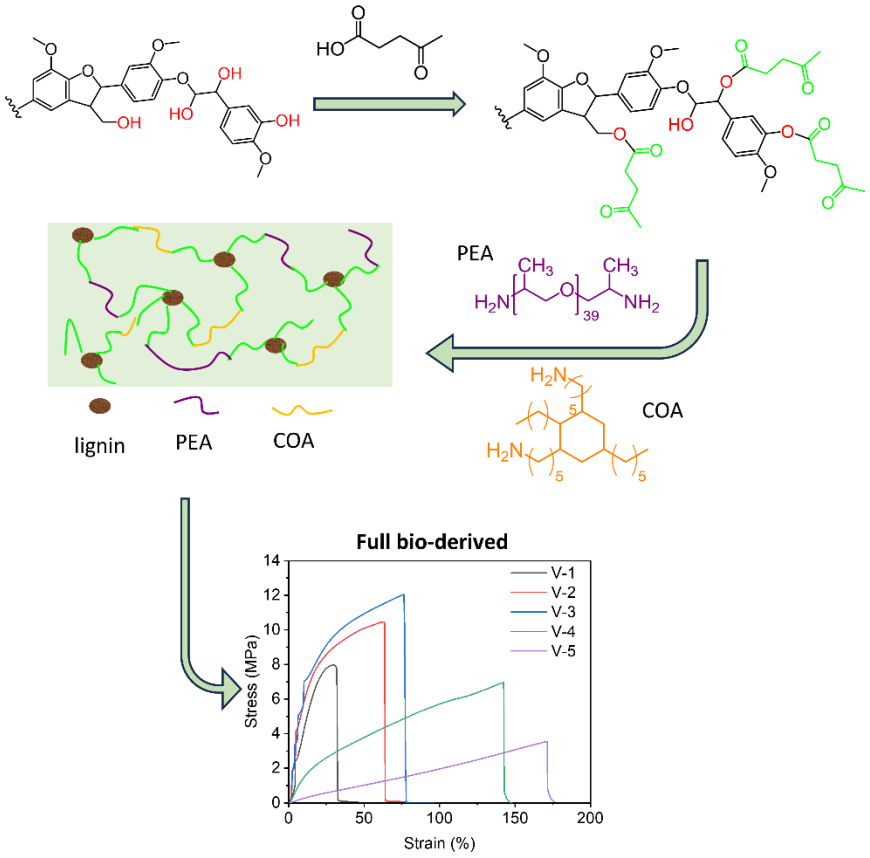

Lignin-based Film with Tunable Mechanical Properties Enabled by Polyether Amine Incorporation

Ruige Qi, Fei Song, Lihong Hu,* and Meng Zhang *

To achieve high-value utilization of lignin and develop high bio-based content materials, flexible films were prepared *via* Schiff base reaction of levulinic acid-esterified lignin with castor oil amine and varying amounts of polyether amine (0 to 50 wt.%). The incorporation of polyether amine as a flexible plasticizing component effectively addressed the inherent brittleness of high-lignin-content films, resulting in tunable mechanical properties. Tensile testing showed that V-3 (15% polyether amine) exhibited the highest tensile strength (12.0 MPa) and Young's modulus (7.19 GPa), representing increases of 51% and 318% compared to V-1 (the 0% polyether amine), while maintaining an elongation at break of 75.9%. All films exhibited good thermal stability with T_d 5% above 272 °C. Swelling ratio measurements increased from 109% (V-1) to 209% (V-5), indicating decreasing crosslinking density with higher polyether amine content. Notably, V-3 exhibited a T_g of 35.8 °C. This study demonstrates a simple strategy for tuning the mechanical properties of lignin-based films for potential biomedical and soft robotics applications.

DOI: 10.15376/biores.21.3.8528-8539

Keywords: Flexible films; Valorization of lignin; Swelling; Crosslinking; Mechanical properties

*Contact information: Institute of Chemical Industry of Forest Products, Chinese Academy of Forestry (CAF), Nanjing, 210042, China; *Corresponding authors: zhangmeng@icifp.cn; hlh@icifp.cn*

INTRODUCTION

Lignin is the second most abundant natural polymer on Earth, following cellulose, and it is the largest renewable source of aromatic compounds. It constitutes 15 to 30% of lignocellulosic biomass by weight and is primarily generated as a byproduct of the pulp and paper industry and biorefinery processes (Agnihotri and Horváth 2024; Abolore *et al*. 2025). Globally, over 100 million tons of lignin are produced annually, yet less than 5% is utilized for high-value applications (Balk *et al.* 2023). The vast majority of lignin is burned as low-value fuel for energy recovery, which not only wastes a valuable renewable resource but also contributes to CO_2 emissions and environmental concerns (Bass and Epps 2021). In recent years, the transition toward a sustainable and circular bioeconomy has accelerated, driven by the need to reduce reliance on fossil-based resources and mitigate climate change (Nguyen *et al.* 2025). Within this context, the development of effective strategies for the high-value utilization of lignin has become a priority for both academic research and industrial application (Ji *et al.* 2024; Song *et al.* 2024).

One effective approach to lignin valorization is its incorporation into polymer materials (Xu *et al.* 2026). These lignin-based polymers offer high stiffness and excellent thermal stability owing to their aromatic backbone, making them attractive for rigid packaging and coating applications (Bai *et al.* 2026). However, the same rigid aromatic

backbone also imparts brittleness, resulting in poor flexibility and low elongation at break, which restricts their use in flexible or impact resistant applications (Lin *et al.* 2026). Furthermore, the poor compatibility between lignin and polymer matrices often leads to lignin aggregation and compromised mechanical performance (Liu *et al.* 2019). Considerable efforts have been devoted to addressing these challenges. A common strategy is the introduction of plasticizers or flexible segments, such as polyethylene glycol (PEG) and other polyols, which have been shown to effectively improve the flexibility and elongation of lignin-based materials (Qi *et al.* 2025). For instance, PEG has been demonstrated to increase the elongation at break of lignin polymers from 16% to over 50% while simultaneously enhancing tensile strength. Hyperbranched poly(ester-amine) and poly(ester-amine-amide) have also been developed as toughening agents for lignin, achieving elastomeric materials with tensile strengths of 12 to 14 MPa and elongations up to 149% (Sivasankarapillai *et al.* 2011, 2012).

Other approaches include incorporating lignin into polyurethane elastomers to form ordered hard domains *via* covalent and non-covalent assembly, achieving a tensile strength of 60.4 MPa and elongation of 532% (Li *et al.* 2025). Preparing lignin/polybutylene succinate composites through reactive extrusion resulted in an 18-fold enhancement in elongation at break (Yan *et al.* 2025). In addition, acetylation modification has been used to improve lignin dispersion in polymer matrices (Peng *et al.* 2025). Despite these advances, systematic investigations into the effect of flexible segment content on the structure-property relationships of lignin-based polymer networks remain limited. Moreover, many of these strategies require high-temperature processing (often above 100 °C) or complex multi-step modifications (De Haro *et al.* 2021). In contrast, the proposed polyether amine toughening strategy is simple and energy-efficient, as the Schiff-base reaction between ketones and amines proceeds readily at room temperature, offering advantages in process simplicity and sustainability.

To address the brittleness of lignin-based materials, this study proposed a polyether amine toughening strategy. Kraft lignin was first esterified with levulinic acid to introduce ketone groups. The resulting esterified lignin (EKL) was then crosslinked with soybean oil amine and varying proportions of polyether amine D2000 *via* Schiff base reaction. Notably, all crosslinking reactions were carried out at room temperature without external heating. The flexible ether linkages of polyether amine are expected to enhance segmental mobility and improve lignin-matrix compatibility, thereby toughening the resulting networks. The effect of polyether amine content on the mechanical and thermal properties was systematically investigated. The results showed that the formulation with 15 wt.% polyether amine exhibited optimal tensile strength and a glass transition temperature T_g of 35.8 °C. Leveraging the photothermal conversion capability of lignin, these materials show promise for soft robotics and medical hot compress applications.

EXPERIMENTAL

Materials

The kraft lignin used in this study is a commercial product derived from mixed softwood (primarily pine and spruce), as supplied by Shanghai Changfa New Materials Co., Ltd. from industrial black liquor.

Levulinic acid (99%), N,N'-dicyclohexyl-carbodiimide (DCC), and 4-dimethylaminopyridine (DMAP) were purchased from Aladdin Biochemical Technology

Co., Ltd. (Shanghai, China). Priamine™ 1075 (COA, dimer fatty acid diamine, total amine 208 mg KOH/g) was kindly provided by Cargill. Polyether amine D2000 (PEA), tetrahydrofuran (THF) and N,N-dimethylformamide (DMF) were obtained from Shanghai Macklin Biochemical Technology Co., Ltd. and used as received.

Preparation of Modified Lignin (EKL)

Acetylated lignin (EKL) was synthesized by esterifying kraft lignin with levulinic acid using DCC as a coupling agent and DMAP as a catalyst in anhydrous DMF. The reaction was carried out at room temperature for 48 h under nitrogen. After filtering off the DCU by-product, the product was precipitated in ice-cold water, washed, and dried under vacuum at 50 °C for 24 h, yielding EKL as a brown powder. The detailed synthesis and characterization methods are described elsewhere (Qi *et al.* 2025).

Preparation of Lignin-based Films

Lignin-based films (VLs, V-1 to V-5) were prepared *via* Schiff base reaction between EKL and mixed diamines. EKL and the diamines (COA and PEA in varying ratios) were separately dissolved in THF, then combined and stirred at room temperature for 2 h (Huang *et al.* 2019). The mixture was left overnight to evaporate most of the solvent, followed by vacuum drying at 60 °C for 12 h to remove residual THF. The resulting prepolymer was hot-pressed at 150 °C under 30 bar for 30 min to obtain dense films. The feed ratios are listed in Table 1.

Table 1. Formulation of Lignin-Based Films

Sample	Modified Lignin		COA		PEA-2000		COA:PEA	Lignin Ratio
	g	mmol C=O	g	mmol NH_2	g	mmol NH_2	mol:mol	Wt.%
V-1	5	17.7	5.31	19.47	0	0	100:0	48.5
V-2	5	17.7	5.23	18.5	0.97	0.97	95:5	44.6
V-3	5	17.7	4.68	16.55	2.92	2.92	85:15	39.7
V-4	5	17.7	3.71	13.63	5.84	5.84	70:30	34.0
V-5	5	17.7	2.65	9.74	9.74	9.74	50:50	28.8

Characterization

Fourier transform infrared (FTIR) spectra were recorded on a Nicolet iS50 spectrometer (Nicolet Instrument Corp., USA) in the range of 4000 to 400 cm^{-1}. ^1H NMR spectra were acquired on a Bruker Avance III 300 MHz spectrometer using DMSO-d_6 as the solvent, with pentafluorobenzaldehyde as an internal standard for quantitative determination of ketone group content in EKL. The molecular weight and dispersity of lignin samples were determined by gel permeation chromatography (GPC) using THF as the eluent and polystyrene standards for calibration.

Thermogravimetric analysis (TGA) was conducted on a STA449F5 instrument (NETZSCH, Germany) under nitrogen atmosphere from room temperature to 800 °C at a heating rate of 20 °C·min^{-1}.

Dynamic mechanical analysis (DMA) was performed on a [instrument model] at a frequency of 1 Hz and a heating rate of 3 °C·min^{-1} over a temperature range of -50 °C to 100 °C to determine the storage modulus (E'), loss modulus (E''), and glass transition temperature (T_g, from tanδ peak).

Tensile properties were measured using a universal testing machine (model, manufacturer, city, country) according to ASTM D638 (Type V). Tests were performed at room temperature with a crosshead speed of 10 mm/min. Tensile strength, Young's modulus, and elongation at break were calculated from the stress-strain curves. At least five specimens were tested for each sample, and the average values with standard deviations are reported.

Swelling ratio and gel content were determined using THF as the solvent. For swelling measurement, dry samples (approximately 0.3 g, W_1) were immersed in THF at 25 °C for 24 h. After removing surface solvent, the swollen weight (W_2) was recorded, and the swelling ratio (Q) was calculated as $Q = (W_2 - W_1)/W_1 \times 100\%$. For gel content measurement, dry samples (approximately 0.3 g, W_1) were extracted with boiling THF in a Soxhlet apparatus for 24 h. The residual samples were dried under vacuum at 50 °C for 24 h, and the final weight (W_2) was recorded. The gel content (G) was calculated as $G = W_2/W_1 \times 100\%$.

RESULTS AND DISCUSSION

Molecular Design and Characterizations of Modified Lignin

The modification of lignin and the synthesis of VLs are schematically illustrated in Fig. 1. FTIR spectroscopy (Fig. 1b) showed that the hydroxyl peak (3200 to 3400 cm^{-1}) and carboxyl peak (1690 to 1710 cm^{-1}) of lignin largely disappeared after esterification, while new peaks corresponding to ester groups (1735 to 1750 cm^{-1}) and ketone groups (1715 to 1725 cm^{-1}) emerged (Derkacheva and Sukhov 2008). GPC analysis (Table 2) indicated that the number-average molecular weight (M_n) of the high molecular weight fraction of esterified lignin increased from 726 to 1739.

Subsequently, using pentafluorobenzaldehyde as an internal standard, the ketone group content of EKL was quantitatively determined by ^{1}H NMR to be 3.54 mmol/g (Fig. 1c). The disappearance of the hydroxyl peak and the appearance of the ester peak confirmed the occurrence of the esterification reaction; the increase in molecular weight indicated that levulinic acid was successfully grafted onto the lignin backbone, resulting in an increased hydrodynamic volume. Collectively, these results demonstrate the successful esterification of lignin with levulinic acid. The appearance of an imine bond absorption peak (1640 to 1650 cm^{-1}) in the FTIR spectrum of the films confirmed its successful synthesis (Xie *et al*. 2024).

Table 2. GPC Data of KL and EKL

	M_n (g / mol)	M_w (g / mol)	PD
KL	726	2271	3.13
EKL	1739	4383	2.52

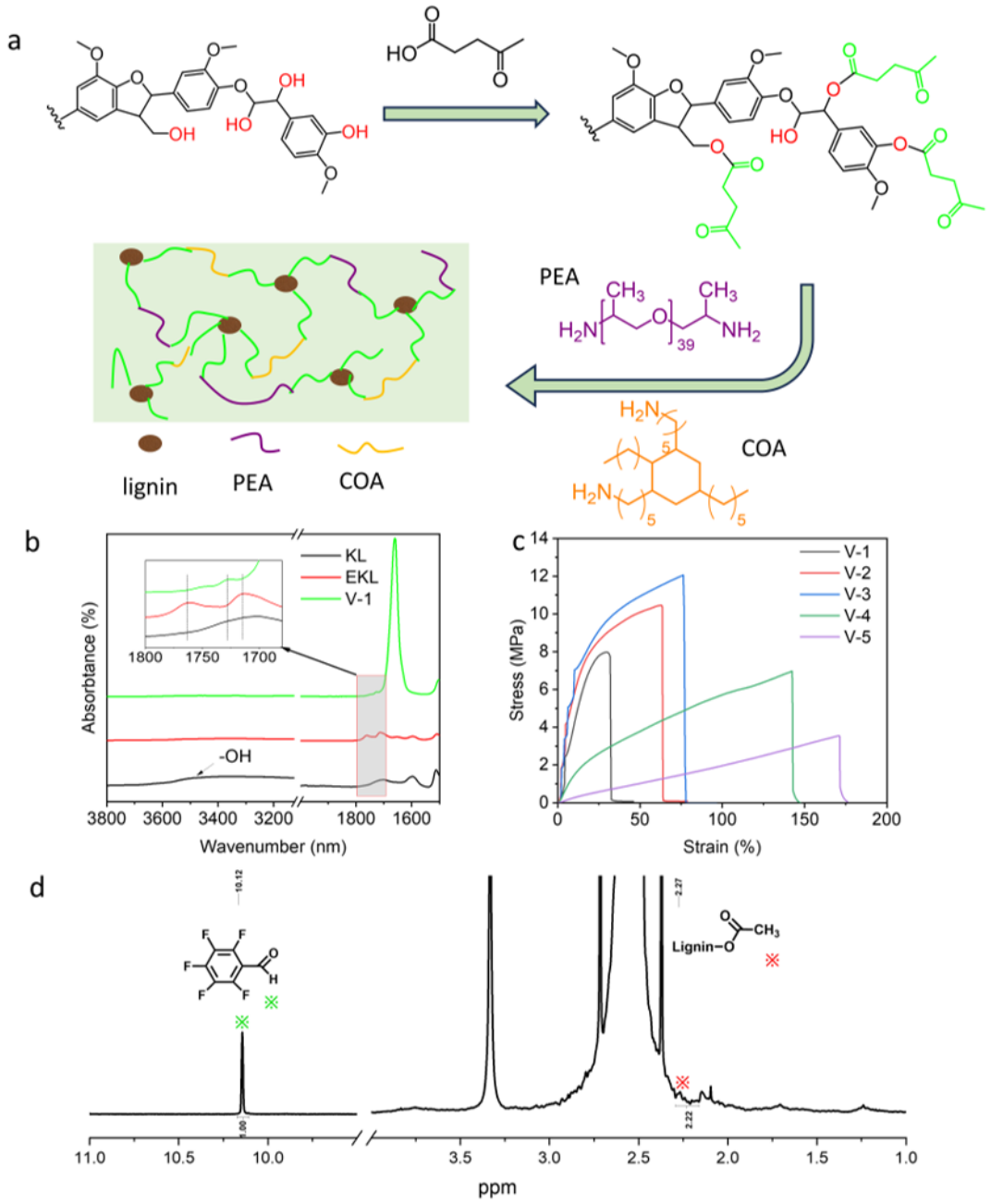

Fig. 1. (a) Schematic illustration of lignin modification and VLs synthesis. (b) FTIR curves of KL, EKL, and V-1. (c) Tensile properties of VLs. (d) The ^{1}H NMR curve of EKL

Mechanical Properties of VLs

As shown in Fig. 1d and Table 3, with increasing polyether amine content, the tensile strength and Young's modulus initially increased and then decreased, while the elongation at break showed a continuous increasing trend. Specifically, V-3 exhibited the highest tensile strength of 12.04 MPa and the highest Young's modulus of 7.19 GPa, representing increases of 51% and 318%, respectively, compared to V-1 (7.95 MPa and 1.72 GPa). Meanwhile, the elongation at break increased from 33.1% (V-1) to 75.9% (V-3).

The improvement in mechanical properties at low replacement ratios (5 to 15%) can be attributed to the flexible nature of the polyether amine chains. The rotational mobility of the ether (-O-) linkages along the polyether backbone has been found to enhance the segmental mobility of the polymer network, leading to increased toughness (Bartels *et al.* 2016). Additionally, the introduction of polyether amine improved the compatibility between the lignin filler and the matrix, resulting in more efficient stress transfer and thus higher tensile strength and modulus (Georgs *et al.* 2025). However, when the replacement ratio exceeded 15% (V-4 and V-5), a further increase in polyether amine content led to a decline in tensile strength (6.97 MPa and 3.50 MPa, respectively) and Young's modulus (6.28 GPa and 2.98 GPa, respectively), accompanied by a dramatic increase in elongation at break (142.6% and 171.2%, respectively). This trend suggests that excessive polyether amine incorporation resulted in a less rigid network structure due to the reduced crosslinking density. The longer and more flexible polyether chains act as plasticizers, promoting ductile deformation but compromising the load-bearing capacity of the material (Lazaro-hdez *et al.* 2025). The optimal mechanical performance was achieved with V-3 (15% replacement), which demonstrated a balanced enhancement of strength, stiffness, and toughness. This composition represents the best compromise between rigid lignin-derived crosslinks and flexible polyether segments.

Table 3. Mechanical Properties Data of VLs

Sample	Tensile strength (MPa)	Elongation at break (%)	Yong's Modulus (GPa)
V-1	7.95±0.84	33.11±5.61	1.72
V-2	10.43±1.12	63.34±4.35	5.21
V-3	12.04±1.58	75.92±10.25	7.19
V-4	6.97±1.44	142.64±9.54	6.28
V-5	3.50±0.59	171.18±15.95	2.98

Thermal Properties

The thermal stability of the raw materials (KL, EKL, PEA, COA) and the resulting films (V-1 to V-5) were evaluated by TGA and DTG, and the results are presented in Fig, 2, with key parameters summarized in Table 4. As shown in Figs. 2a and 2b and Table 2, KL exhibited a T_d of 223.6 °C and a T_{dmax} of 382.4 °C, with a high char residue of 39.14% at 600 °C due to its aromatic backbone. After esterification with levulinic acid, EKL showed lower thermal stability, with T_d decreasing to 193.5 °C and T_{dmax} to 329.6 °C, along with a reduced char residue of 27.5%. This decrease can be attributed to the introduction of thermally labile ester linkages during the esterification reaction (Khan *et al.* 2021). In contrast, the two amine monomers exhibited distinctly different thermal behaviors. COA displayed a T_d of 267.3 °C and a T_{dmax} of 360.5 °C with a slightly negative char residue (-2.07%), indicating near-complete decomposition. PEA demonstrated the highest thermal stability among all raw materials, with a T_d of 300.8 °C and a T_{dmax} of 363.6°C, leaving a negligible char residue (-0.85%). The superior thermal stability of PEA is attributed to the stable ether (-O-) linkages along its polyether backbone.

As the polyether amine replacement ratio increased from 0% to 50%, the T_d values of the films increased progressively from 272.1°C (V-1) to 311.1 °C (V-5), indicating enhanced thermal stability upon PEA incorporation (Fig. 2d,e). The T_{dmax} initially increased from 458.4 °C (V-1) to 459.9 °C (V-2), then gradually decreased to 401.5 °C (V-5). Notably, all films exhibited significantly higher T_{dmax} values (401 to 460 °C) compared to their raw material counterparts (329 to 383 °C), suggesting that the crosslinked network

structure substantially improved thermal stability. The significant drop in T_{dmax} for V-4 and V-5 (405.7 °C and 401.5 °C, respectively) suggests a change in the degradation mechanism at higher PEA loadings (≥30%), which was likely due to the preferential decomposition of the more labile polyether segments. The char residue at 600 °C ranged from 11.0% to 15.4%, with no clear trend observed with increasing PEA content. All films showed positive char residues (11 to 15%), in contrast to the neat amines, confirming the formation of a crosslinked network with enhanced char-forming capacity.

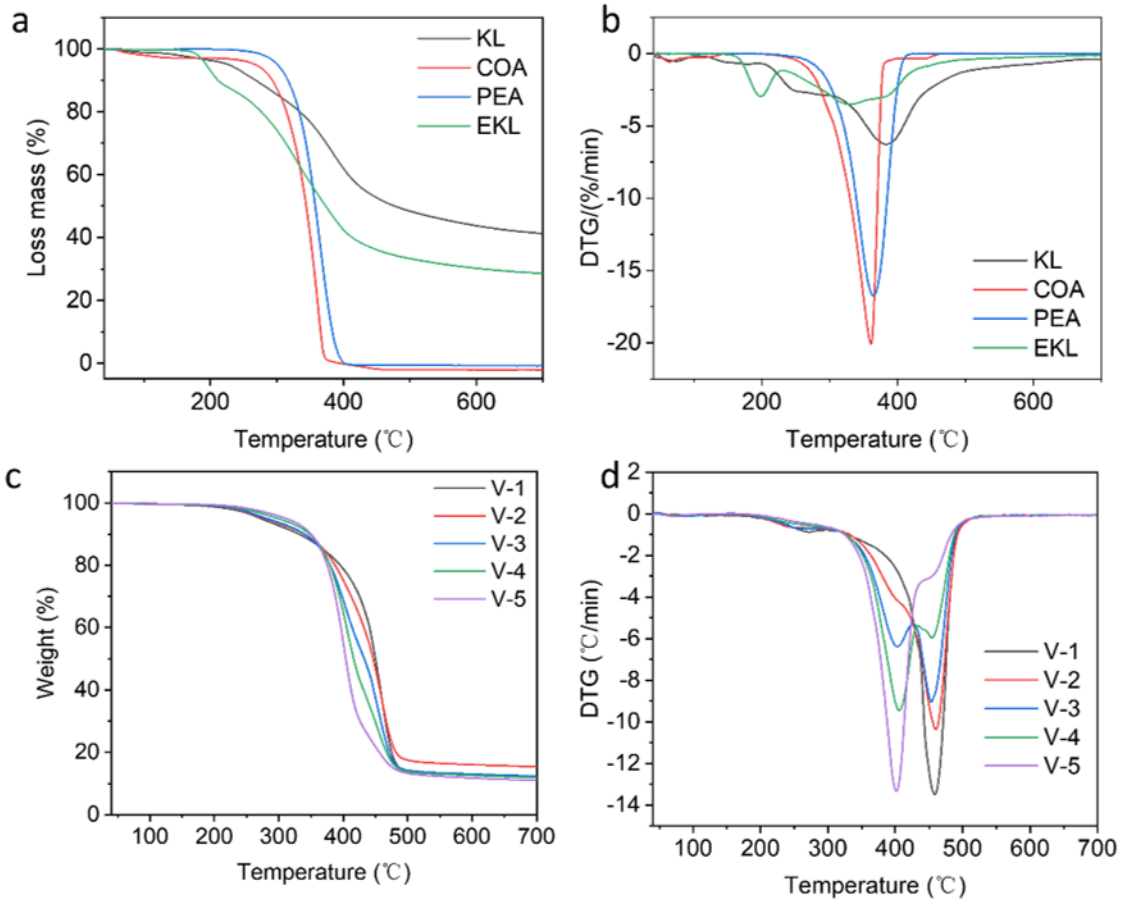

Fig. 2. (a,b) TG and DTG curves of KL, COA, PEA, and EKL. (c,d) TG and DTG curves of VLs

Table 4. Thermal Data of Samples

Sample name	T_d (5%, ℃)	T_{dmax} (max first derivative) (℃)	Residue TGA (%)
KL	223.6	382.4	39.14
EKL	193.5	329.6	27.48
COA	267.3	360.5	-2.07
PEA	300.8	363.6	-0.85
V-1	272.1	458.4	11.95
V-2	279.1	459.9	15.37
V-3	281.1	453.7	12.35
V-4	299.1	405.7	11.94
V-5	311.1	401.5	11.07

Dynamic Mechanical Properties of VLs

The viscoelastic behavior of the films (V-1 to V-5) was investigated by DMA. The storage modulus (E'), loss factor (tanδ), and loss modulus (E'') curves are presented in Fig. 3, and the key parameters are summarized in Table 5. As shown in Fig. 4a and Table 3, the storage modulus at 25 °C decreased dramatically with increasing PEA content, from 368.14 MPa (V-1) to 7.07 MPa (V-5), indicating that PEA effectively reduced the stiffness of the film. This trend is consistent with the Young's modulus values obtained from tensile testing (Section 3.2). At the glass transition temperature, V-3 exhibited the highest E' at T_g (28.8 MPa), suggesting that this formulation maintained greater structural integrity at the transition temperature, which may contribute to its superior tensile strength.

The glass transition temperatures determined from the tanδ peaks (Fig. 3b) decreased progressively with increasing PEA content from 58.2 °C to -8.1 °C (V-5). This decrease is attributed to the plasticizing effect of the flexible PEA segments, whose ether linkages enhance segmental mobility and increase free volume (Wang *et al.* 2022). Notably, V-5 exhibited a T_g below 0 °C, indicating a transition to a rubbery state at room temperature, consistent with its high elongation at break (171%) and low tensile strength (3.50 MPa). The tanδ peak height and full width at half maximum (FWHM) are also summarized in Table 3. All samples exhibited broad FWHM values (76.8 to 81.8 °C), indicating highly heterogeneous network structures characteristic of lignin-based materials. V-1 showed the highest peak height (0.67), indicating the strongest damping response at its T_g.

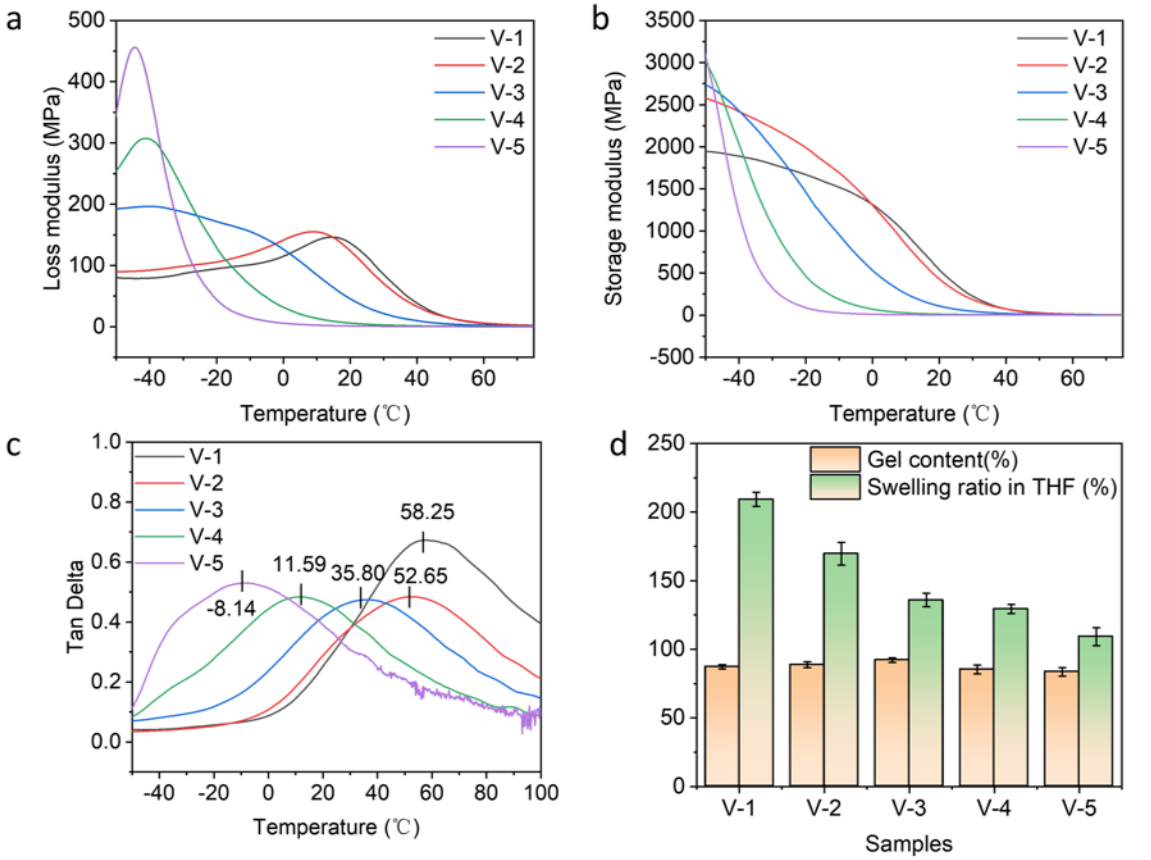

Fig. 3. (a,b,c) Loss modulus, Storage Modulus, and tanδ curves of VLs. (d) Gel content and swelling ratio in THF of VLs

The loss modulus curves (Fig. 3c) provided additional insight into the relaxation behavior. V-1 and V-2 exhibited broad *E″* peaks at approximately 20 °C and 8.9 °C, respectively. Remarkably, V-3 (15% PEA) displayed an unusually broad E" profile without a distinct peak, confirming a highly heterogeneous network structure. This unique relaxation behavior correlates with the superior mechanical performance of V-3, which exhibited the highest tensile strength (12.04 MPa) among all formulations. In contrast, V-4 and V-5 showed sharp, well-defined *E″* peaks at -41.33 °C and -44.37 °C, respectively, indicating a transition to more homogeneous rubbery networks at high PEA loadings.

Table 5. Dynamic Mechanical Properties of VLs

Sample name	*E'* at 25 ℃	*E'* at T_g	*E'* at T_g +30 ℃	T_g from tanδ (°C)	FWHM (℃)	*E''* peak temperature (℃)
V-1	368	9.23	1.21	58.2	81.8	20
V-2	287	22.9	4.17	52.6	78.9	8.9
V-3	73.8	28.8	4.68	35.8	76.8	No distinct peak
V-4	11.6	24.5	4.03	11.6	78.4	-41.3
V-5	7.07	23.3	2.85	-8.1	81.2	-44.4

Swelling and Gel Content of VLs

The gel content and swelling ratio of the VLs were determined by Soxhlet extraction using THF as the solvent. The samples were extracted for 24 h, and the results are summarized in Fig. 3d. All VLs exhibited high gel contents ranging from 83.5% to 92.0%, indicating successful formation of a crosslinked network. The gel content increased from 87.3% (V-1) to a maximum of 92.0% (V-3), then decreased to 83.5% (V-5). This suggests that an appropriate amount of PEA (up to 15%) promoted more complete crosslinking, while excessive PEA led to a less complete network.

The swelling ratio in THF increased progressively with PEA content, from 109% (V-1) to 209% (V-5). A higher swelling ratio indicates lower crosslinking density. This trend is consistent with the DMA results: V-1 exhibited the lowest swelling ratio and highest T_g (58.2 °C), while V-5 showed the highest swelling ratio and lowest T_g (-8.14 °C). V-3 achieved an intermediate swelling ratio (135%) while exhibiting the highest tensile strength (12.0 MPa) and gel content, demonstrating that an optimal crosslinking density exists for balancing strength and toughness.

CONCLUSIONS

1. The optimal formulation (V-3, 15% polyether amine) exhibited the highest tensile strength (12.04 MPa) and Young's modulus (7.19 GPa), with a T_g of 35.8 °C.
2. All films showed good thermal stability (T_d > 272 °C) and solvent resistance. Leveraging the photothermal conversion capability of lignin and the tunable T_g.
3. This work offers a simple strategy for the high-value utilization of lignin.

ACKNOWLEDGMENTS

The authors of this work acknowledge the financial support of Fundamental Research Funds of CAF (CAFYBB2023QD001-05) and the National Key Research and Development Program Project (2023YFD2201903-3).

Declaration of Competing Interest

The authors declare that they have no known competing financial interests or personal relationships that could have appeared to influence the work reported in this paper.

Data Availability

Data will be made available on request.

REFERENCES CITED

Abolore, R. S., Jaiswal, S., and Jaiswal, A. K. (2025). "A comprehensive review on sustainable lignin extraction techniques, modifications, and emerging applications," *Industrial Crops and Products* 235, article 121696. https://doi.org/10.1016/j.indcrop.2025.121696

Agnihotri, S., and Horváth, I. S. (2024). "Integrated products biorefinery options within the Swedish pulp and paper industry: Current status," *Sustainable Chemistry for the Environment* 7, article 100128. https://doi.org/10.1016/j.scenv.2024.100128

Bai, D., Shi, L., Li, C., Xiao, T., Huang, L., Wu, L., and Shi, H. (2026). "Advances in lignin-based polyurethane elastomers and their multifunctional applications," *ACS Applied Polymer Materials* 8(8), 5364-5396. https://doi.org/10.1021/acsapm.6c00102

Balk, M., Sofia, P., Neffe, A. T., and Tirelli, N. (2023). "Lignin, the lignification process, and advanced lignin-based materials," *International Journal of Molecular Sciences* 24(14), article 11668. https://doi.org/10.3390/ijms241411668

Bartels, J., Wang, J.-H. H., Chen, Q., Runt, J., and Colby, R. H. (2016). "Segmental dynamics of ethylene oxide-containing polymers with diverse backbone chemistries," *Macromolecules* 49(5), 1903-1910. https://doi.org/10.1021/acs.macromol.5b02423

Bass, G. F., and Epps, T. H. (2021). "Recent developments towards performance-enhancing lignin-based polymers," *Polymer Chemistry* 12(29), 4130-4158. https://doi.org/10.1039/D1PY00694K

de Haro, J. C., Tatsi, E., Fagiolari, L., Bonomo, M., Barolo, C., Turri, S., Bella, F., and Griffini, G. (2021). "Lignin-based polymer electrolyte membranes for sustainable aqueous dye-sensitized solar cells," *ACS Sustainable Chemistry & Engineering* 9(25), 8550-8560. https://doi.org/10.1021/acssuschemeng.1c01882

Derkacheva, O., and Sukhov, D. (2008). "Investigation of lignins by FTIR spectroscopy," *Macromolecular Symposia* 265(1), 61-68. https://doi.org/10.1002/masy.200850507

Georgs, V., Piili, H., Gustafsson, J., and Xu, C. (2025). "A critical review on lignin structure, chemistry, and modification towards utilisation in additive manufacturing of lignin-based composites," *Industrial Crops and Products* 233, article 121416. https://doi.org/10.1016/j.indcrop.2025.121416

Huang, K., Ma, S., Wang, S., Li, Q., Wu, Z., Liu, J., Liu, R., and Zhu, J. (2019). "Sustainable valorization of lignin with levulinic acid and its application in polyimine thermosets," *Green Chemistry* 21, 4964-4970. http://doi.org/10.1039/C9GC02384D.

Ji, D., Wang, Y., Peng, J., Yuan, D., Li, Z., Ji, D., and Wu, H. (2024). "Recent advances in depolymerization and high-value utilization of lignin: A review," *Industrial & Engineering Chemistry Research* 63(46), 19916-19935. https://doi.org/10.1021/acs.iecr.4c02617

Khan, Z., Javed, F., Shamair, Z., Hafeez, A., Fazal, T., Aslam, A., Zimmerman, W. B., and Rehman, F. (2021). "Current developments in esterification reaction: A review on process and parameters," *Journal of Industrial and Engineering Chemistry* 103, 80-101. https://doi.org/10.1016/j.jiec.2021.07.018

Lazaro-Hdez, C., Valerga, A. P., Gomez-Carturla, J., Sanchez-Nacher, L., Boronat, T., and Ivorra-Martinez, J. (2025). "Optimization of the ductile properties of poly(lactic acid) (PLA) using green citrate-based plasticizers and itaconic anhydride grafted PLA (PLA-g-IA)," *International Journal of Biological Macromolecules* 307, article 142034. https://doi.org/10.1016/j.ijbiomac.2025.142034

Li, Z., Hong, H., Wu, H., Wang, D., Liu, L., Puchalski, M., and Yao, J. (2025). "Lignin defined ordered hard domains toward mechanically robust, long-term weather resistant bio-elastomer," *International Journal of Biological Macromolecules* 318, article 144895. https://doi.org/10.1016/j.ijbiomac.2025.144895

Lin, L., Cao, W., Liu, H., Zhou, Z., Wang, H., Chen, Q., Pu, X., Kuzhandaivel, D., Weng, Z., and Wu, L. (2026). "Synthesis of an aromatic polyester for enhanced mechanical properties of stereolithography resins," *Reactive and Functional Polymers* 221, article 106656. https://doi.org/10.1016/j.reactfunctpolym.2026.106656

Liu, W., Fang, C., Wang, S., Huang, J., and Qiu, X. (2019). "High-performance lignin-containing polyurethane elastomers with dynamic covalent polymer networks," *Macromolecules* 52(17), 6474-6484. https://doi.org/10.1021/acs.macromol.9b01413

Nguyen, T. H., Wang, X., Utomo, D., Gage, E., and Xu, B. (2025). "Circular bioeconomy and sustainable food systems: What are the possible mechanisms?" *Cleaner and Circular Bioeconomy* 11, article 100145. https://doi.org/10.1016/j.clcb.2025.100145

Peng, X., Jiang, F., and Li, Z. (2025). "Enhancing compatibility of polylactic acid and lignin through acetylation for improving controlled release of pesticide," *Pest Management Science* 81(6), 3088-3102. https://doi.org/10.1002/ps.8677

Qi, R., Zhang, M., Xue, Y., Hu, L., Bo, C., Zhou, Y., and Wang, H. (2025). "Multiresponsive shape memory photothermal elastomers based on unmodified and high-content lignin," *International Journal of Biological Macromolecules* 328(Pt 2), article 147533. https://doi.org/10.1016/j.ijbiomac.2025.147533

Sivasankarapillai, G., and McDonald, A. G. (2011). "Synthesis and properties of lignin-highly branched poly(ester-amine) polymeric systems," *Biomass and Bioenergy* 35(2), 919-931. https://doi.org/10.1016/j.biombioe.2010.11.002

Sivasankarapillai, G., McDonald, A. G., and Li, H. (2012). "Lignin valorization by forming toughened lignin-co-polymers: Development of hyperbranched prepolymers for cross-linking," *Biomass and Bioenergy* 47, 99-108. https://doi.org/10.1016/j.biombioe.2012.09.057

Song, T., He, H., Li, X., Liu, X., Lv, Y., Tao, Y., Lu, J., Du, J., Hu, J., and Wang, H. (2024). "A green strategy to realize the high value utilization of lignin for hydrogel formation," *Science of the Total Environment* 955, article 176760. https://doi.org/10.1016/j.scitotenv.2024.176760

Wang, S., Luo, Z., Liang, J., Hu, J., Jiang, N., He, J., and Li, Q. (2022). "Polymer nanocomposite dielectrics: Understanding the matrix/particle interface," *ACS Nano* 16(9), 13612-13656. https://doi.org/10.1021/acsnano.2c07404

Xie, D., Pu, Y., Bryant, N. D., Harper, D. P., Wang, W., Ragauskas, A. J., and Li, M. (2024). "Synthesis of bio-based repairable polyimines with tailored properties by lignin fractionation," *ACS Sustainable Chemistry & Engineering* 12, 6606-6618, http://doi:10.1021/acssuschemeng.3c08482.

Xu, Y.-C., Zou, S.-L., Wang, Q., and Xiao, L.-P. (2026). "Lignin upgrading for sustainable materials and chemicals: From waste to functional bioplastics," *Bioresource Technology* 445, article 134091. https://doi.org/10.1016/j.biortech.2026.134091

Yan, Q., Xue, B., Zhao, Q., Wang, W., Li, X., Zhao, Y., Wen, J., Meng, X., and Zhao, W. (2025). "Fully biobased, ultra-tough lignin/polybutylene succinate composites through reactive extrusion," *Industrial Crops and Products* 226, article 120638. https://doi.org/10.1016/j.indcrop.2025.120638

Article submitted: May 13, 2026; Peer review completed: June 8, 2026; Revised version received: June 19, 2026; Accepted: July 20, 2026; Published: July 27, 2026.
DOI: 10.15376/biores.21.3.8528-8539